Global NEST Journal, Vol 19, No 1, pp 160-166

Effects of V_2O_5 and WO_3 loadings on the catalytic performance of V_2O_5-WO_3/TiO_2 catalyst for SCR of NO with NH_3

Tao P., Sun M.H., Qu S.C., Song C.W.*, Li C., Yin Y.Y. and Cheng M.R.
College of Environmental Science and Engineering, Dalian Maritime University, 1 Linghai Road, Dalian 116026, China
Received: 20/07/2016, Accepted: 09/11/2016, Available online: 29/03/2017
*to whom all correspondence should be addressed:
e-mail: chengwensong@dlmu.edu.cn

Abstract

V_2O_5-WO_3/TiO_2 catalysts were fabricated by a simple impregnation method. Effects of V_2O_5 and WO_3 loadings on the catalytic performance of V_2O_5-WO_3/TiO_2 catalyst for selective catalytic reduction (SCR) of NO with NH_3 were investigated. Morphology and structure of the V_2O_5-WO_3/TiO_2 catalysts were characterised by XRD, SEM, XPS, and N_2 adsorption techniques. The XRD patterns of the V_2O_5-WO_3/TiO_2 catalyst are indexed to anatase-TiO_2. XPS spectra analysis confirms that V, Ti, W and O species exist on the surface of V_2O_5-WO_3/TiO_2 catalyst. V_2O_5 species are the main active sites in the process of SCR reaction. Increasing V_2O_5 loading in the V_2O_5-WO_3/TiO_2 catalysts can improve their catalytic performance. Exceeding 2 wt%, the catalytic performance of V_2O_5-WO_3/TiO_2 catalyst begins to decline because high V_2O_5 loading on TiO_2 speeds up the growth of anatase grains, which leads to the loss of catalytic activity. Appropriate WO_3 species can significantly improve the catalytic performance of V_2O_5-WO_3/TiO_2 catalysts. However, as the WO_3 loadings reaches 6 wt%, NO conversion decreases instead.

Keywords: V_2O_5-WO_3/TiO_2 catalyst; SCR; Impregnation methods; Chemisorbed oxygen

1. Introduction

Nitrogen oxides (NO_x), as major atmospheric pollutants (Yu *et al.*, 2013; Liu *et al.*, 2014), have caused a series of environmental issues, such as ozone depletion, acid rain, photochemical smog, particulate matters (PM2.5) transformation, greenhouse effect etc (Skalska *et al.*, 2010; Kompio *et al.*, 2012; Yang *et al.*, 2014; Huang *et al.*, 2015; Ma *et al.*, 2015). In recent years, with the significant growth of environmental awareness, the environmental problems arising from nitrogen oxides (NO_x) have been paid more attention. Facing the rising social dissatisfaction with the state of the environment, Governments, especially in Europe, Japan, the United States and China (Gao *et al.*, 2013; Jiang *et al.*, 2016), have enacted a series of stringent emission regulations. Also, many researchers develop various promising technologies, such as NO_x storage and reduction (NSR), the lean NO_x trap (LNT), and selective catalytic reduction (SCR) of NO_x with ammonia, to solve those issues. Among these methods, NSR usually requires a large amount of fuel to create a reductive atmosphere. LNT is relatively simple and efficient, but it needs expensive platinum group metal (PGM) (Herreros *et al.*, 2014; Gu *et al.*, 2015; Raptotasios *et al.*, 2015; Seo *et al.*, 2015; Wang *et al.*, 2015;). SCR is considered to be the most efficient technology due to its high efficiency, selectivity and economy, and becomes the leading NO_x control strategy for decades (Shakya *et al.*, 2015; Zhang *et al.*, 2015).

Many catalysts have been reported to be adopted for the SCR reaction, such as loaded V, Cu, Fe and Mn species over TiO_2, Al_2O_3, AC and zeolites supports (Leistner and Olsson, 2015; Usbertia *et al.*, 2015; Romero-Sáez *et al.*, 2016). The most important catalyst currently used for SCR is based on V_2O_5-WO_3/TiO_2 catalyst because it has a relatively high activity and N_2 selectivity at 300-400 °C. Up to now, many works on the preparation of V_2O_5-WO_3/TiO_2 catalysts and their application on the selective catalytic reduction (SCR) of NO with NH_3 were reported. Rodella and Mastelaro investigated the influence of the vanadium load and calcination temperature on the structural characteristics of the V_2O_5/TiO_2 system obtained by the sol–gel method, and proved it is useful to modify the structure of the V_2O_5/TiO_2 system by adjusting different amounts of vanadium and calcination temperatures (Rodella and Mastelaro, 2003). Kobayashi and Hagi reported their work on the V_2O_5-WO_3 catalysts loaded on the Ti-rich TiO_2-SiO_2-SO_4^{2-} by the coprecipitation method, and clarified the effect of active components and supports on activities in the selective catalytic reduction of NO by NH_3 (Kobayashi and Hagi, 2006). Djerad *et al.,* synthesized V_2O_5-WO_3/TiO_2 catalysts by the sol–gel method, and found the catalytic behavior of V_2O_5-WO_3/TiO_2 catalyst is strongly dependent on V_2O_5 content (Djerad *et al.*, 2004). Dong *et al.,* investigated the effect of the pH value of vanadium precursor solution on the catalytic performance of V_2O_5-WO_3/TiO_2 catalysts through wet impregnation, and indicated that high de-NO_x activity of the V_2O_5-WO_3/TiO_2 catalysts can be obtained by enhancing the precursor solution acidity in the preparation process (Dong *et al.*, 2014). Pang *et al.,* demonstrated that ultrasound-assisted impregnation method can promote the strong interaction between the V_2O_5 and TiO_2-WO_3 support and stabilize V_2O_5 in the reduced state (Pang *et al.*,

2014). Zhang *et al.,* fabricated the V_2O_5-WO_3/TiO_2 catalyst by a sol–gel method, and investigate the interaction of V, W and Ti species for the improvement of the catalytic activity in the SCR reaction. They found that WO_3 could interact with TiO_2 to improve the electrons transfer, and the WO_3 hybridization with V_2O_5 could also improve the reducibility and formation of reduced V_2O_5 species (Zhang *et al.*, 2015). These previous studies have shown that the catalytic properties of V_2O_5-WO_3/TiO_2 catalysts are markedly influenced by some parameters, such as preparation methods and conditions, concentration of the active component etc. In this study, we synthesized V_2O_5-WO_3/TiO_2 catalysts using a simple impregnation method, investigated the morphology and structure characteristics of the V_2O_5-WO_3/TiO_2 catalysts by XRD, SEM, XPS, and N_2 adsorption techniques, and further illustrated the effects of V_2O_5 and WO_3 loadings on the catalytic performance of V_2O_5-WO_3/TiO_2 catalyst in the selective catalytic reduction (SCR) of NO with NH_3.

2. Experimental

2.1. Preparation of V_2O_5-WO_3/TiO_2 catalyst

The V_2O_5-WO_3/TiO_2 catalyst was prepared by impregnation method. Sodium Tungstate Dihyrate (Na_2WO_4) (WO_3 loadings were 1 wt%, 3 wt%, and 6 wt%, respectively) and 0.96 g oxalic acid ($H_2C_2O_4$) were dissolved in 6.8 mL deionized water under magnetic stirring until they completely dissolved. Then 8 g commercial anatase TiO_2 powder was added into the above solution under stirring for 2 h at room temperature. After that, the above mixture was dried at 80 °C for 12 h, and then it was grinded and subsequently calcined at 450 °C for 4h. Ammonium metavanadate (NH_4VO_3) (V_2O_5 loadings were 0.5 wt%, 1.5 wt%, and 2 wt %, respectively) and 0.248 g oxalic acid were completely dissolved in 6.8 ml deionized water under magnetic stirring at room temperature. After TiO_2-WO_3 powder was introduced in the solution under stirring for 2 h, the above mixture was dried at 80 °C for 12 h. Then it was grinded and subsequently calcined at 450 °C for 4 h. Finally, the V_2O_5-WO_3/TiO_2 powder was obtained, which was referred as Vx%TiWy%. For example, V1.5%TiW6% meant the catalyst with 1.5 wt% V_2O_5 and 6 wt% WO_3 loadings.

2.2. Catalytic activity measurement

The activity measurements were carried out in a fixed-bed quartz reactor which contained 4.00 g catalysts of 20 mesh and 1.15 g quartz sand (another 1.15 g quartz sand to control air velocity). The feed gas mixture contained 0.05 vol % NO, 0.08 vol % NH_3, 2.5 vol% O_2 and balanced N_2 at a flow rate of 330 ml min^{-1} controlled by mass flow meters. The reaction temperature was increased to 550 °C in a heating rate of 5 °C min^{-1}. The NO conversion was calculated by testing the NO concentration at the inlet and outlet of reactor according to China National Standard (GB/T 8969-1988).

2.3. Characterization

X-ray diffraction (XRD) patterns of V_2O_5-WO_3/TiO_2 catalysts were recorded using a D/Max-2400 diffractometer (Cu Kα radiation, λ =1.54055 Å) in a range of diffraction angle 2θ from 10 º to 80 º to analyze the diffraction peaks of V_2O_5-WO_3/TiO_2 catalysts. The pore structure properties of V_2O_5-WO_3/TiO_2 catalysts was characterized by using a Quantachrome Autosorb-iQ automated gas adsorption system with liquid nitrogen (at 77 K). The morphology of V_2O_5-WO_3/TiO_2 catalysts was observed by a Philips XL30 FEG scanning electron microscope (SEM). X-ray photoelectron spectroscopy (XPS) of V_2O_5-WO_3/TiO_2 catalysts was carried out on a Thermo Scientific ESCALAB 250 spectrometer with a monochromation Al Ka source.

3. Results and discussion

3.1. Effect of V_2O_5 loadings on the catalytic performance of V_2O_5-WO_3/TiO_2 catalyst

Fig. 1 shows the typical XRD patterns of V_2O_5-WO_3/TiO_2 catalysts at different V_2O_5 loadings. All the diffraction peaks (2θ=25.44 °, 38.10 °, 48.17 °, 54.38 °, 55.13 °, 62.75 °, 70.48 °, 75.30°) are indexed to anatase-TiO_2 (PDF#21-1272) (Zhang *et al.*, 2015). In addition, we also notice that the crystalline phase of V_2O_5 is not detected in all the XRD patterns, which may be attributed to low amounts of V_2O_5 in these catalysts, and thus no obvious diffraction peaks are observed. Furthermore, there are almost no significant differences on diffraction peaks with the increase of V_2O_5 loadings. Therefore, we can conclude that the particle size and crystal phase have little change by V_2O_5 loadings.

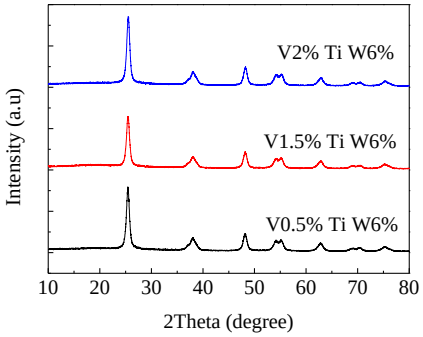

Figure 1. XRD patterns of V_2O_5-WO_3/TiO_2 catalyst at different V_2O_5 loadings

Fig. 2 depicts the high-resolution spectra of V2p, W4f, Ti2p and O1s, which suggests that these species exist on the surface of V_2O_5-WO_3/TiO_2 catalyst. As shown in Fig. 2a, three kinds of V species can be distinguished in the V2p spectrum. The binding energies at 514.88 eV, 516.08 eV and 516.98 eV are attributed to $V^{3+}2p_{2/3}$, $V^{4+}2p_{2/3}$ and $V^{5+}2p_{2/3}$, respectively, and V mainly exists as the V^{+5} oxidation state on the V_2O_5-WO_3/TiO_2 catalyst (Li *et al.*, 2015). Fig. 2b presents the $W4f_{7/2}$ and $W4f_{5/2}$ peaks in the XPS spectra, which are located at 36.18 eV and 37.48 eV, respectively, indicating the W^{6+} oxidation state. Fig. 2c shows the XPS spectra for Ti2p of V_2O_5-WO_3/TiO_2 catalyst. The two peaks at 464.18 and 458.58 eV are ascribed to $Ti2p_{1/2}$ and $Ti2p_{3/2}$, respectively, suggesting that Ti exists as the Ti^{+4} state.

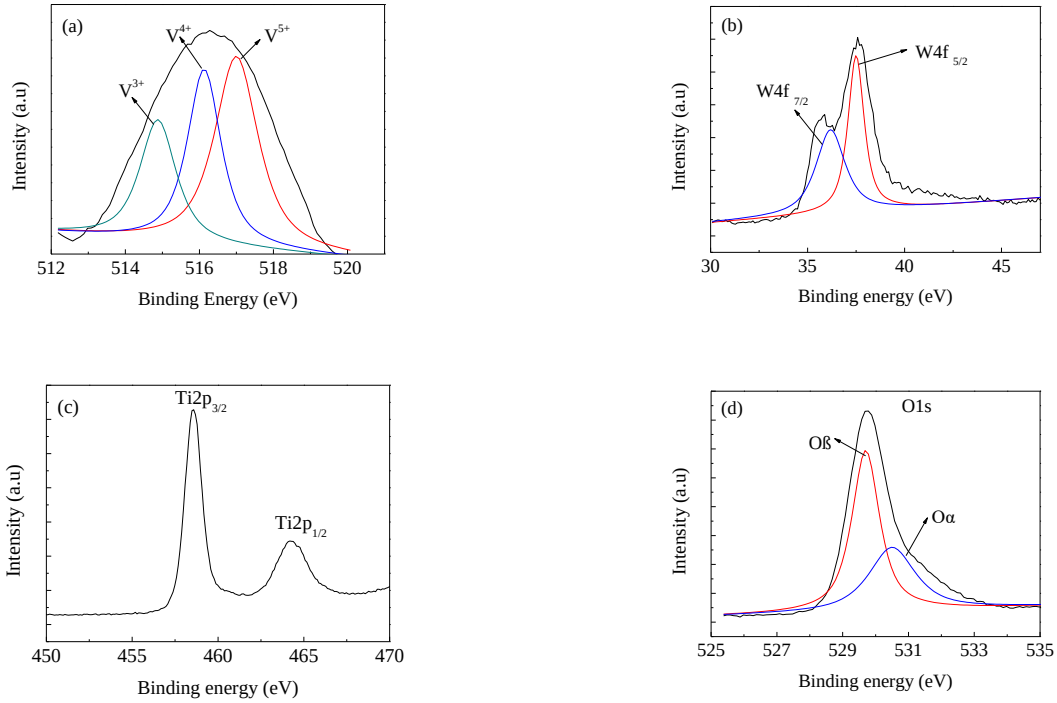

Figure 2. XPS spectra of V_2O_5-WO_3/TiO_2 catalysts: (a) V2p spectrum, (b) W4f spectrum, (c) Ti2p spectrum, and (d) O1s spectrum

Fig. 2d shows the O1s peaks of V_2O_5-WO_3/TiO_2 catalyst which can be fitted into two peaks. The binding energy at 529.68 eV 530.48 eV are referred to as the lattice oxygen (Oβ) and the chemisorbed surface oxygen (Oα), respectively (Ref 24). Generally, the chemisorbed surface oxygen (Oα) has a significant effect on the deep oxidation reactions of reducing substances. Therefore, the presence of the chemisorbed surface oxygen (Oα) will be beneficial to the SCR reaction. Fig. 3 is the typical SEM images of as-prepared V_2O_5-WO_3/TiO_2 catalysts at different V_2O_5 loadings (0.5 wt%, 1.5 wt%, and 2 wt%). The particles of V_2O_5-WO_3/TiO_2 catalysts show the sphere-like morphology with ranging from 30 to 50 nm. These spherical particles condense to form agglomerates. There are no apparent differences between the V_2O_5-WO_3/TiO_2 catalysts with 0.5 wt% and 1.5 wt% V_2O_5 loadings. As for 2 wt% V_2O_5 loading, the aggregations of catalytic particles are slightly serious.

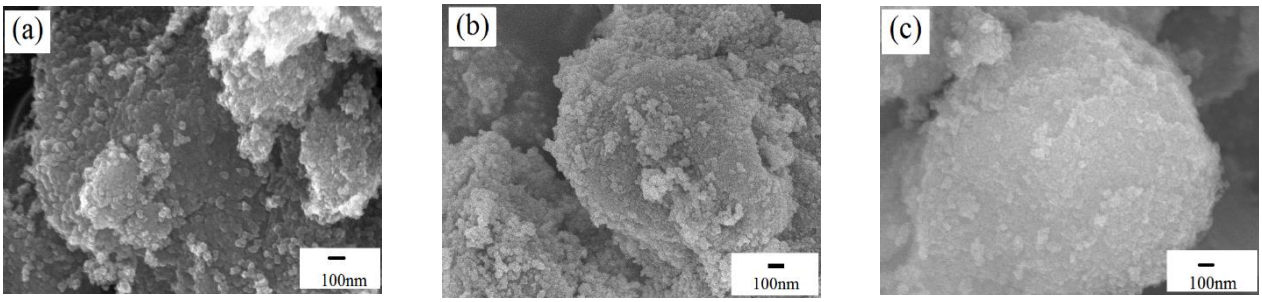

Figure 3. SEM images of V_2O_5-WO_3/TiO_2 catalysts: (a) V0.5%TiW6%, (b) V1.5%TiW6%, (c) V2%TiW6%

Fig. 4 shows NO conversion for the V_2O_5-WO_3/TiO_2 catalysts at different V_2O_5 loadings as a function of temperature from 100 to 550 °C. Obviously, the NO conversion for all the prepared catalysts increases significantly with increasing reaction temperature below 300 °C and then reaches a steady state. When the reaction temperature is above 400 °C, the NO conversion begins to decrease. Among these catalysts, the two catalysts without V_2O_5 loadings (TiW1% and TiW6%) demonstrate low catalytic activity and narrow active windows. When V_2O_5 species are loaded, the catalytic performance of the catalysts is significantly improved, and the maximal catalytic activity and widest active window (250 °C~500 °C) are achieves at 1.5 wt% of V_2O_5 loadings. All those imply that V_2O_5 species are the active sites on the V_2O_5-WO_3/TiO_2 catalyst because they can decrease the activation energy of SCR reaction (Amiridis and Solar, 1996; Busca *et al.*, 1998). However, further increasing V_2O_5 loading to 2 wt%, the catalytic performance of the catalysts declines instead. The phenomenon may be attributed to that high V_2O_5 loadings

on TiO_2 speed up the growth of anatase-TiO_2 grains, which leads to the loss of catalytic activity (Wang *et al.*, 2016). Therefore, the V_2O_5 loading of 1.5 wt% is recommended for NO conversion by V_2O_5-WO_3/TiO_2 catalyst.

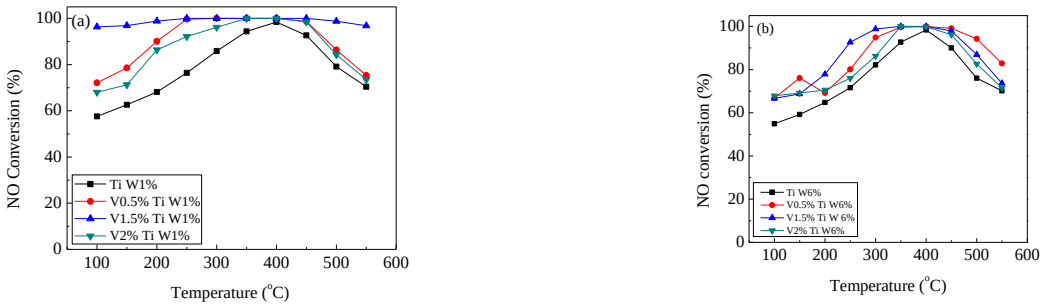

Figure 4. NO conversion for the V_2O_5-WO_3/TiO_2 catalysts with (a) 1 % WO_3 loading, (b) 6 % WO_3 loadings at different V_2O_5 loadings

3.2. Effect of WO_3 loadings on the catalytic performance of V_2O_5-WO_3/TiO_2 catalyst

Fig. 5 provides the XRD patterns of V_2O_5-WO_3/TiO_2 catalysts at different WO_3 loadings. Similarly, only diffraction peaks assigned to anatase-TiO_2 (PDF#21-1272) are observed and diffraction peaks indexed to WO_3 are also not detected in the XRD patterns due to low WO_3 amount. Besides, there are no significant change on diffraction peak with the increase of WO_3 loadings, which implies that the particle size and crystal phase have little change by changing the WO_3 loadings. Fig. 6 shows the XPS spectra of W4f, V2p, Ti2p and O1s, which approves that these species exist on the surface of V_2O_5-WO_3/TiO_2 catalyst.

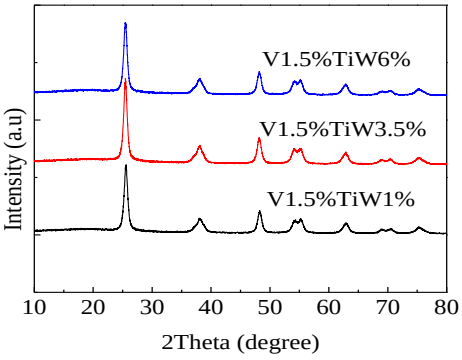

Figure 5. XRD patterns of V_2O_5-WO_3/TiO_2 catalyst at different WO_3 loadings

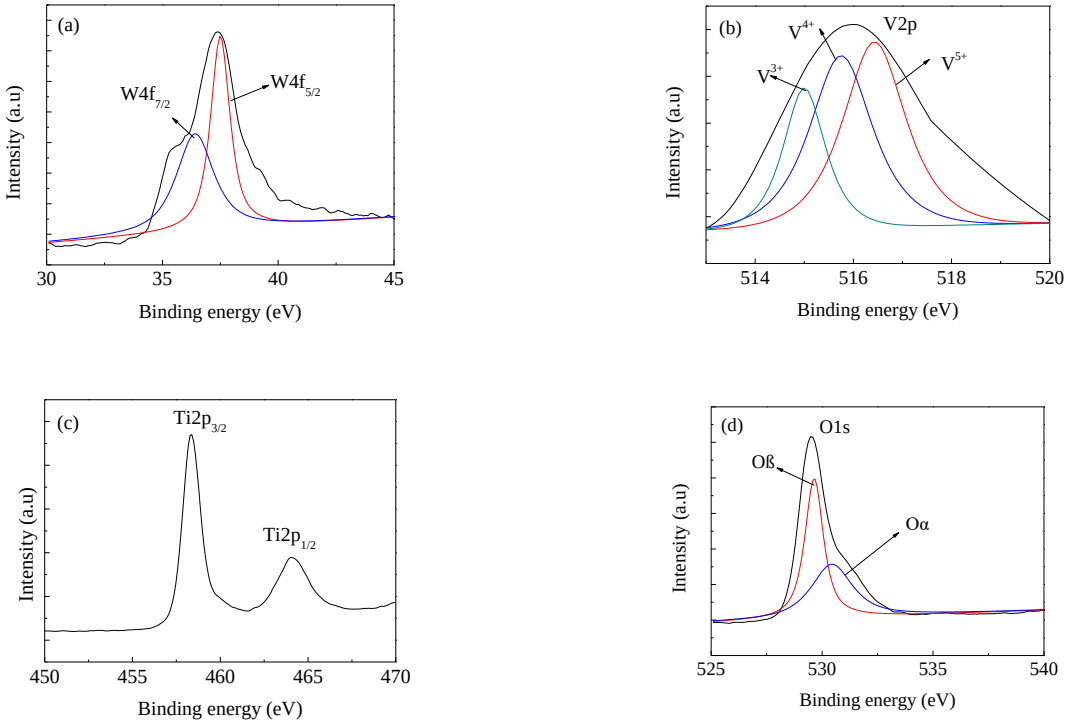

Figure 6. XPS spectra of V_2O_5-WO_3/TiO_2 catalyst: (a) W4f spectrum, (b) V2p spectrum, (c) Ti2p spectrum, (d) O1s spectrum

As shown in Fig. 6a, the binding energies at 37.48 and 36.38 eV are attributed to $W^{6+}4f_{5/2}$ and $W^{6+}4f_{7/2}$, respectively. Fig. 6b presents the information that three kinds of surface V species can be distinguished in the V2p spectrum. It is clear that the binding energies at 514.98, 515.78 and 516.48 eV are attributed to $V^{3+}2p_{2/3}$, $V^{4+}2p_{2/3}$ and $V^{5+}2p2/3$, respectively, and V^{+5} state mainly exists on the V_2O_5-WO_3/TiO_2 catalyst. The two peaks at 464.08 and 458.38 eV are ascribed to $Ti^{4+}2p_{1/2}$ and $Ti^{4+}2p_{3/2}$, respectively (Fig. 6c). Fig. 6d shows the O1s peaks of V_2O_5-WO_3/TiO_2 catalyst which can be fitted into two peaks. The binding energy at 529.68 eV is referred as the lattice oxygen (Oβ) while at 530.48eV is referred to as the chemisorbed surface oxygen (Oα). As we known, surface chemisorbed oxygen has been reported to be the most active oxygen and plays an important role in oxidation reactions. Therefore, high ratio of Oα/(Oα+Oβ) on the catalyst surface may also be related to a high SCR activity (Chen *et al.*, 2011). As shown in Fig. 6d and Fig. 2d, the ratio of Oα/(Oα+Oβ) of V1.5%TiW3.5% is higher than that in V1.5%TiW6% which indicates that V1.5%TiW3.5% has a better catalytic performance than V1.5%TiW6%. Fig. 7 shows the SEM images of V_2O_5-WO_3/TiO_2 catalysts fabricated at different WO_3 loadings (1 wt%, 3.5 wt%, and 6 wt%). The spherical catalytic particles are obviously agglomerated from the SEM images, which sizes are uniform. There are no apparent differences between the three V_2O_5-WO_3/TiO_2 catalysts. Fig. 8 presents the adsorption-desorption isotherms of V_2O_5-WO_3/TiO_2 catalyst, which demonstrates typical type Ⅳ curve with the hysteresis loop. The BET surface area is calculated to be 30.07 $m^2 g^{-1}$, which shows a facilitation effect toward the SCR reaction.

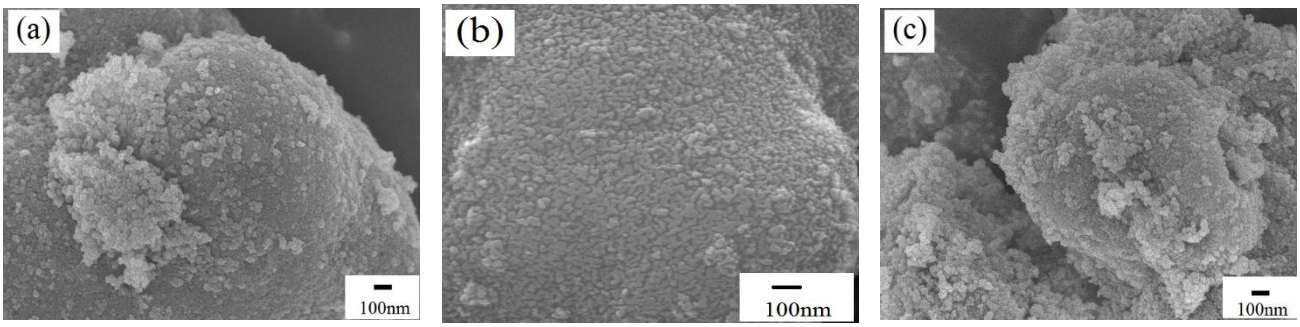

Figure 7. SEM images of V_2O_5-WO_3/TiO_2 catalyst: (a) V1.5%TiW1%, (b) V1.5%TiW3.5%, (c) V1.5%TiW6%

Fig. 9 shows NO conversion for the V_2O_5-WO_3/TiO_2 catalysts at different WO_3 loadings as a function of temperature from 100 to 550 °C. When the catalyst without WO_3 loading (V1.5%Ti) is adopted, the NO conversion is only 70.86% at 200 °C, and decreases significantly above 400 °C, which indicates its low catalytic activity and narrow temperature window. When the WO_3 loadings in the catalyst are 1 wt% and 3.5 wt%, the NO conversion of the prepared catalysts increase to 98.86 % and 98.53 % at 200 ◦C, and almost no NO can be detected above 250 °C (250–450 °C). This is because that the WO_3 species improve the electrons transfer of the V_2O_5-WO_3/TiO_2 catalyst, which results in the increase of the superoxide ions, prompting the SCR reaction. Increasing WO_3 loadings in the catalyst to 6 wt%, the NO conversion increases with the increase of reaction temperature below 300 °C, and then it dramatically decreases. The catalyst shows low catalytic activity and the NO conversion is only 77.88 % and 73.65 % at 200 °C and 550 °C, respectively. Also, the temperature window of the V_2O_5-WO_3/TiO_2 catalysts at 6 wt% of WO_3 loadings is narrow, which may be ascribed to that excessive WO_3 loadings trap electrons to inhibit the formation of superoxide ions (Zhang and Zhong, 2013).

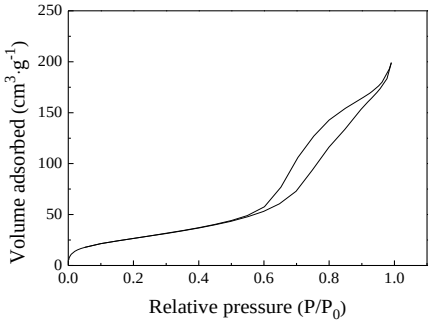

Figure 8. Nitrogen adsorption-desorption isotherms of V_2O_5-WO_3/TiO_2 catalyst

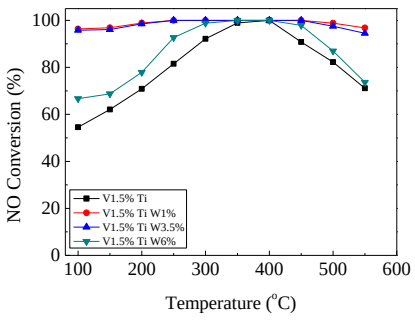

Figure 9. NO conversion for the V_2O_5-WO_3/TiO_2 catalysts at different WO_3 loadings

4. Conclusion

In summary, we report our works on the preparation of V_2O_5-WO_3/TiO_2 catalysts using a simple impregnation method and their application on the selective catalytic reduction (SCR) of NO with NH_3.

Increasing V_2O_5 loading in the V_2O_5-WO_3/TiO_2 catalysts can improve their catalytic activities. However, when V_2O_5 loading exceeds 2 wt%, the activity of V_2O_5-WO_3/TiO_2 catalyst begins to decline because high V_2O_5 loading on TiO_2 speeds up the growth of anatase-TiO_2 grains, which leads to the loss of catalytic activity. With the increase of WO_3 loadings, NO conversion is significantly promoted, however, when the WO_3 loadings reaches 6 wt%, NO conversion decreases instead due to the inhibition on the formation of superoxide ions.

Acknowledgement

This work was supported by the National Natural Science Foundation of China (21276035, 21476034), the Scientific Research Project of Education Department of Liaoning Province (L2013203), the Natural Science Foundation of Liaoning Province (2014025014), the Science and Technology Foundation for Overseas Chinese Scholars, Ministry of Human Resources and Social Security of China, and the Fundamental Research Funds for the Central Universities (3132016327).

Reference

Amiridis M.D. and Solar J.P. (1996), Selective Catalytic Reduction of Nitric Oxide by Ammonia over V_2O_5/TiO_2, V_2O_5/TiO_2/SiO_2, and V_2O_5-WO_3/TiO_2 Catalysts: Effect of Vanadia Content on the Activation Energy, *Ind. Eng. Chem. Res*, **35**, 978-981.

Busca G., Lietti L., Ramis G. and Berti F. (1998), Chemical and mechanistic aspects of the selective catalytic reduction of NO_x by ammonia over oxide catalysts: A review, *Appl. Catal. B: Environ,* **18**, 1-36.

Chen L., Li J.H. and Ge M.F. (2011), The poisoning effect of alkali metals doping over nano V_2O_5–WO_3/TiO_2 catalysts on selective catalytic reduction of NOx by NH_3, *Chem. Eng. J*, **170**, 531–537.

Djerad S., Tifouti L., Crocoll M. and Weisweiler W. (2004), Effect of vanadia and tungsten loadings on the physical and chemical characteristics of V_2O_5-WO_3/TiO_2 catalysts, *J. Mol. Catal. A: Chem.*, **208**, 257–265.

Dong G.J., Zhang Y.F., Zhao Y. and Bai Y. (2014), Effect of the pH value of precursor solution on the catalytic performance of V_2O_5-WO_3/TiO_2 in the low temperature NH_3-SCR of NOx, *J. Fuel. Chem. Technol*, **42**, 1455-1463.

Gao Y., Luan T., Lv T., Cheng K. and Xu H.M. (2013), Performance of V_2O_5-WO_3-MoO_3/TiO_2 Catalyst for Selective Catalytic Reduction of NO*x* by NH_3, *Chinese. J. Chem. Eng*, **21**, 1-7.

Gu H., Chun K.M. and Song S. (2015), The effects of hydrogen on the efficiency of NOx reduction via hydrocarbon-selective catalytic reduction (HC-SCR) at low temperature using various reductants, *Int. J. Hydrogen. Energ,* **40**, 9602-9610.

Herreros J.M., George P., Umar M. and Tsolakis A. (2014), Enhancing selective catalytic reduction of NOx with alternative reactants/promoters, *Chem. Eng. J.*, **252**, 47–54.

Huang X.M., Zhang S.L., Chen H.N. and Zhong Q. (2015), Selective catalytic reduction of NO with NH_3 over V_2O_5 supported on TiO_2 and Al_2O_3: A comparative study, *J. Mol. Struct*, **1098**, 289-297.

Jiang K., Geng P., Meng F. and Zhang H. (2016), An extended Kalman filter for input estimations in diesel-engine selective catalytic reduction applications, *Neurocomputing*, **171**, 569–575.

Kobayashi M. and Hagi M. (2006), V_2O_5-WO_3/TiO_2-SiO_2-SO_4^{2-} catalysts: Influence of active components and supports on activities in the selective catalytic reduction of NO by NH_3 and in the oxidation of SO_2, *Appl.Catal. B: Environ.*, **63**, 104–113.

Kompio P.G.W.A., Brückner A., Hipler F., Auer G., Löffler E. and Grünert W. (2012), A new view on the relations between tungsten and vanadium in V_2O_5-WO_3/TiO_2 catalysts for the selective reduction of NO with NH_3, *J. Catal.*, **286**, 237–247.

Leistner K. and Olsson L. (2015), Deactivation of Cu/SAPO-34 during low-temperature NH3-SCR, *Appl. Catal. B: Environ,* **165**, 192–199.

Li Z.G., Li J.H., Liu S.X., Ren X.N., Ma J., Su W.K. and Peng Y. (2015), Ultra hydrothermal stability of CeO_2-WO_3/TiO_2 for NH_3-SCR of NO compared to traditional V_2O_5-WO_3/TiO_2 catalyst, *Catal. Today*, **258**, 11-16.

Liu Z.M., Zhang S.X., Li J.H., Zhu J.Z. and Ma L.L. (2014), Novel V_2O_5–CeO_2/TiO_2 catalyst with low vanadium loading for the selective catalytic reduction of NO_x by NH_3, *Appl. Catal. B: Environ,* **158–159**, 11–19.

Ma Z.R., Wu X.D., Si Z.S., Weng D., Ma J. and Xu T.F. (2015), Impacts of niobia loading on active sites and surface acidity in NbOx/CeO_2–ZrO_2 NH_3–SCR catalysts, *Appl. Catal. B: Environ,* **179**, 380–394.

Pang L., Fan C., Shao L., Yi J.X., Cai X., Wang J., Kang M. and Li T. (2014), Effect of V_2O_5/WO_3-TiO_2 catalyst preparation method on NOx removal from diesel exhaust ,*Chinese. J. Catal*, **35**, 2020-2028.

Raptotasios S.I., Sakellaridis N.F., Papagiannakis R.G. and Hountalas D.T. (2015), Application of a multi-zone combustion model to investigate the NOx reduction potential of two-stroke marine diesel engines using EGR, *Applied Energy,* **157**, 814-823.

Rodella C.B. and Mastelaro V.R. (2003), Structural characterization of the V_2O_5/TiO_2 system obtained by the sol–gel method, *J. Phys. Chem. Solids*, **64**, 833–839.

Romero-Sáez M., Divakar D., Aranzabal A., González-Velasco J.R. and González-Marcos J.A. (2016), Catalytic oxidation of trichloroethylene over Fe-ZSM-5: Influence of the preparation method on the iron species and the catalytic behavior, *Appl. Catal. B: Environ,* **180**, 210–218.

Seo C.K. and Choi B. (2015), Physicochemical characteristics according to aging of Fe-zeolite and V_2O_5–WO_3–TiO_2 SCR for diesel engines*, J. Ind. Eng. Chem,* **25**, 239–249.

Shakya B.M., Harold M.P. and Balakotaiah V. (2015), Simulations and optimization of combined Fe- and Cu-zeolite SCR monolith catalysts, *Chem. Eng. J,* **278**, 374–384.

Skalska K., Miller J.S. and Ledakowicz S. (2010), Trends in NO_x abatement: A review, *Sci.Total Environ.*, **408**, 3976–3989.

Usbertia N., Jablonskab M., Blasic M.D., Forzattia P., Liettia L. and Beretta A. (2015), Design of a "high-efficiency" NH3-SCR reactor for stationary applications, a kinetic study of NH_3 oxidation and NH_3-SCR over V-based catalysts, *Appl. Catal. B: Environ,* **179**, 185–195.

Wang C., Li X., Xia F., Zhang H. and Xiao J. (2016), Effect of V_2O_5-content on electrode catalytic layer morphology and mixed potential ammonia sensor performance, *Sensor. Actuat. B*, **223**, 658–663.

Wang J.H., Dong X.S., Wang Y.J. and Li Y.D. (2015), Effect of the calcination temperature on the performance of a CeMoOx catalyst in the selective catalytic reduction of NOx with ammonia, *Catal. Today*, **245**, 10–15.

Yang J.C., Sun R., Sun S.Z., Zhao N.B., Hao N., Chen H., Wang Y., Guo H.R. and Meng Jianqiang. (2014), Experimental study on

NO_x reduction from staging combustion of high volatile pulverized coals. Part 1, Air staging. *Fuel. Process. Technol,* **126**, 266–275.

Yu W.C., Wu X.D., Si Z.C. and Weng D. (2013), Influences of impregnation procedure on the SCR activity and alkali resistance of V_2O_5–WO_3/TiO_2 catalyst, *Appl. Surf. Sci,* **283**, 209–214.

Zhang Q.M., Song C.L., Lv G., Bin F., Pang H.T. and Song J.O. (2015), Effect of metal oxide partial substitution of V_2O_5 in V_2O_5–WO_3/TiO_2 on selective catalytic reduction of NO with NH_3, *J. Ind. Eng. Chem*, **24**, 79–86.

Zhang S. and Zhong Q. (2013), Promotional effect of WO_3 on O_2^- over V_2O_5/TiO_2 catalyst for selective catalytic reduction of NO with NH_3, *J. Mol. Struct. Catal. A: Chem*, **373** , 108–113.

Zhang S.L. and Zhong Q. (2015), Surface characterization studies on the interaction of V_2O_5–WO_3/TiO_2 catalyst for low temperature SCR of NO with NH_3, *J. Solid. State. Chem,* **221**, 49–56.